Publ. Natl. Astron. Obs. Japan Vol. 13. 1－8 (2010)

Nonlinearity in the Detector used in the Subaru Telescope High Dispersion Spectrograph

Akito TAJITSU, Wako AOKI, Satoshi KAWANOMOTO, and Norio NARITA

(Received 2009 Oct. 30; accepted 2010 Feb. 11)

Abstract

The nonlinearity of the charge-coupled devices (CCDs) used in the Subaru Telescope High Dispersion Spectrograph (HDS) is investigated. Measurements are performed by using a halogen lamp, whose intensity is sufficiently stable for our purpose, for flat fielding. While good linearity is confirmed in the data recorded for electron numbers less than 10,000e^- (～6,000ADU), significant nonlinearity appears for higher electron numbers. The nonlinearity is of the order of several percent at 50,000e^-. No clear pixel-to-pixel difference is observed in the nonlinearity effect in a given chip; however, there is a notable difference in the nonlinearity effect between two CCD chips used in the instrument. The source of the nonlinearity (CCD chip or the electronics) is not identified in our measurements. No significant time variation in the nonlinearity effect is found from our measurements carried out for two years. The procedure to correct these nonlinearity effects is provided in this paper.

Key words: instrumentation, detectors, spectrographs

1. Introduction

Since its first light in 2000, the High Dispersion Spectrograph (HDS: Noguchi et al. 2002) of the Subaru Telescope has been widely used in various fields of astronomy. The primary targets of the instrument in its construction phase were relatively faint objects such as quasi-stellar objects and Galactic halo stars. However, with the rapid progress made in the observational studies of extrasolar planets in the 2000s, there is a need for detailed measurements of bright objects with a very high signal-to-noise ratio (SNR) within a short exposure time.

One such example is the investigation of stellar light absorption by the atmosphere of a planet around the central star. In such observations, it is necessary to detect small variations in the spectral features with the orbital phase with a very high SNR. In such cases, even small nonlinearities of the CCDs can give rise to significant errors. This is because the CCD counts obtained by individual exposures are not necessarily constant owing to variations in the observational conditions (e.g., atmospheric extinction or transmission). This problem in the Subaru/HDS was investigated by Snellen et al. (2008), who improved the measurement quality by applying empirical corrections for the nonlinearity in the same type of detectors used in other instruments.

The nonlinearity effect is also observed when a spectrum is obtained with insufficient spatial sampling. When the spectrum is recorded with a CCD binned in the spatial (slit) direction under good seeing conditions, the target star is sampled only by one or two (effective) pixels. Such an observation is carried out to increase the time resolution by reducing the CCD readout time. If nonlinearity actually exists, the obtained CCD counts depend strongly on the pixel numbers of the stellar image (typically one or two pixels) (See section 3).

The detector in the HDS is a mosaic (2 by 1) EEV CCD 42-80 with a 4100×2048 format of 13.5-μm pixels. Its control system consists of a CCD front-end circuit named M-front and a CCD controller named Messia-V (Nakaya et al. 2006). Similar nonlinearity effects have been observed in some other instruments that use the above mentioned type of CCD (Wide Field Camera in the Isaac Newton Telescope[1], AF2/WYFFOS [Worswick et al. 1995] in the 4.2-m William Herschel Telescope[2], etc.). Furthermore, in our private communication (Izumiura 2008), a similar phenomenon has been observed in the HIgh Dispersion Echelle Spectrograph (HIDES: Izumiura 1999) at the Okayama Astrophysical Observatory. When this phenomenon was found, HIDES was using the same EEV 42-80 CCDs with the same front-end electronics (M-front) and a similar control system (Messia-III: Sekiguchi et al. 1998).

In this paper, we report our measurement of the nonlinearity of the CCDs used in the HDS. Our measurement techniques are described in section 2. The results are reported in section 3, along with discussions of the nonlinearity characteristics. A correction formula and

[1] http://www.ast.cam.ac.uk/~wfcsur/technical/foibles/

[2] http://www.ing.iac.es/Engineering/detectors/ultra_2eev.htm

correction coefficients are also provided. The summary of the study is given in section 4.

2. Measurement technique

2.1. Instrument setup and measurement accuracy

The HDS is currently mounted on one of the Nasmyth foci of the telescope. This instrument is installed in an enclosure, with only one entrance shutter behind the slit. With the present setup, it is difficult to investigate the performance of the detector unit separately. Therefore, we use a halogen lamp for flat fielding (hereafter "flat") as the standard light source and an entrance shutter to control the exposure during our measurements. In order to reduce the uncertainty in the exposure caused by fluctuations in the halogen lamp intensity and the errors in the shutter opening and shutter closing times, the measurements are carried out using ND filters so that the exposure time is increased.

Measurements are made for standard Echelle spectra for flat fielding using a standard setup named StdI2b, which covers wavelengths of 352≃479 nm and 493≃618 nm, by two mosaiced CCDs, (blue and red CCD respectively). The slit width and slit length are set to 400 μm and 2000 μm respectively. These correspond to 0″.8 and 4″.0 for celestial targets, respectively. Figure 1 shows an example of a spectral image in which the data in the overscan region are removed, corrections for the bias level are made, and ADU counts are converted to electron numbers (= photon numbers) by using the ADC gain (∼1.7 e^-/ADU for each readout port). Such images are obtained by changing the exposure time. All raw images are processed in the same way as an example in figure 1. Therefore, ADU counts in each frame are converted to electron numbers. Hereafter we use such electron numbers as "CCD counts" in our argument.

In order to investigate the stability of the halogen lamp intensity and accuracy of the shutter control, we repeated our measurements for different exposure times. One set of the measurements consists of 16 different exposure times ranging from 5 s to 80 s, and we repeated it 10 times. The stability of our measurement system is shown in figure 2. Electron numbers of flat spectra are measured at a same area of the CCD chip (around position B in figure 1). Then, in order to compare the data obtained with different exposure times, the "relative differences" in the measured numbers among frames with the same exposure times are calculated; these differences are shown as functions of time (modified Julian date [MJD]) and exposure time (left and right panels, respectively) in the figure. The intensity of the lamp becomes sufficiently stable two hours after the lamp is turned on. When the data points obtained in the first two hours (the first four sets of the ten) are excluded, the relative differences among the measured counts show a smaller scatter (filled circles in the right panel). The scatter is slightly larger in the data obtained for an exposure time of 5 s. Hence, we use the data obtained for an exposure time of 10 s or longer. The scatter of the data points indicates that the random error in the measurements is $\lesssim$ 0.1%.

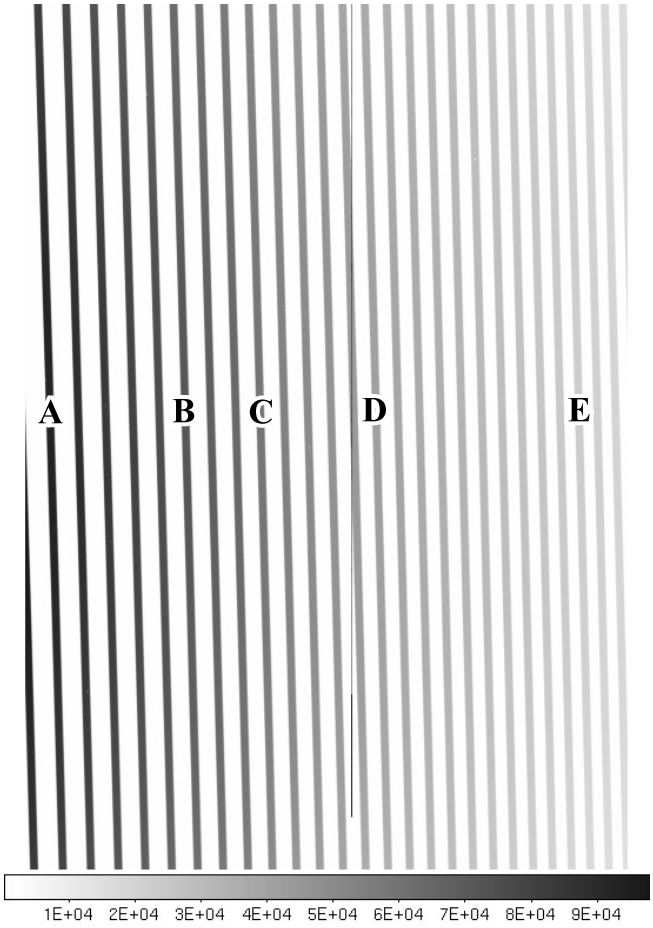

Fig. 1. Example of a two-dimensional CCD image of a flat spectrum (red CCD). The Echelle spectrum of HDS consists of a series of lines with different spectral orders. The wavelength increases from bottom to top in each spectrum and from right to left for each Echelle order. The counts in the flat spectrum have slopes with different orders (increasing from right to left in this example) because of the wavelength dependence of the halogen lamp intensity and the efficiency of the HDS. Measurements are performed in regions A≃E (see text).

Figure 3 shows the electron number for regions A-E in figure 1 as a function of exposure time. The solid lines indicate the linear least-square fits to the data points. Since the electron numbers differ significantly among regions A≃E because of the wavelength dependence of the halogen lamp

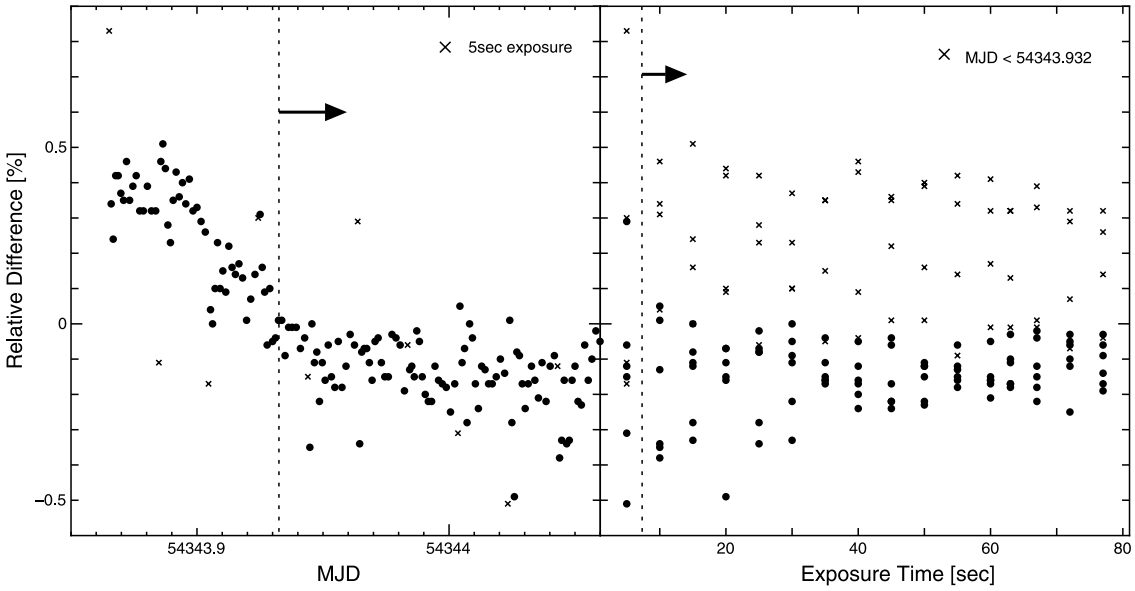

Fig. 2. Relative difference among the counts in the flat spectra obtained at different exposure times for investigating the stability of the intensity of the halogen lamp and the shutter opening and shutter closing times. The left panel shows the results as functions of measurement time (MJD: modified Julian date), while the right panel depicts the results as a function of exposure time.

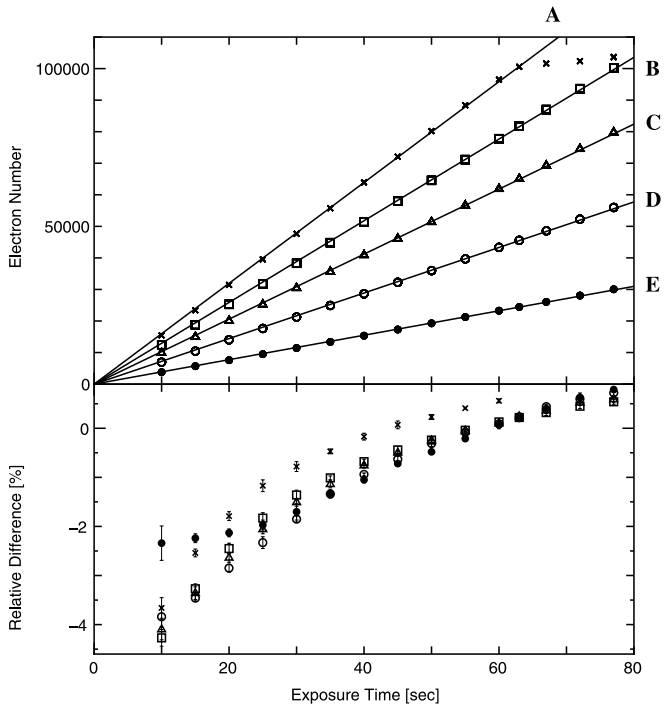

Fig. 3. Correlation between signal counts and exposure times. The upper panel shows electron numbers as functions of exposure time for the five regions mentioned in figure 1. The solid lines indicate linear fits to the data points. Saturation effect is observed in Region A when electron number exceeds 100,000e$^-$. The lower panel shows the departure from the linear fit. Error bars show the standard deviations of the last six of the ten measurements.

intensity and the spectrograph efficiency, the slopes of the electron number vs. exposure time plots are different. The lower panel shows the departure from the linear fit, which is 4% at the most. Above 100,000e$^-$, region A shows a saturation effect corresponding to the saturation of the 16-bit A/D converter.

2.2. Measurements at two exposure times

Such measurements made at many different exposure times are time-consuming in data acquisition as well as for data analysis. This is significant when measurements are repeated several times for investigating the dependence of the nonlinearity on the CCD chips and the binning modes, as well as time variations in the nonlinearity effect.

In order to measure the nonlinearity effect more efficiently, we adopt a different measurement technique in which the large variations in the CCD counts in each spectral image are taken into account. This approach is based on the assumption that the nonlinearity effect is not dependent on the pixels in each CCD chip. It is difficult to confirm this assumption on the basis of the measurements reported in the previous section alone, as the departures from perfect linearity at each measurement point have similar slopes. However, this assumption is justified during the following measurement.

In our private communication with the HIDES developer, we came to know that a clear relationship exists between the apparent CCD counts and the ratio of the counts at different exposure times (Izumiura 2008). By taking into account this

fact, we use two spectral images obtained at two different exposure times (30 s and 60 s) in our new approach. In order to verify the stability of the halogen lamp intensity and to increase the statistical reliability, we repeat the measurements 10 times. Then, we obtain an averaged spectral image for each exposure time. The counts, which are the electron numbers converted from the raw ADU counts, in the image obtained at an exposure time of 30 s are doubled and subtracted from those in the image obtained for an exposure time of 60 s. Figure 4 shows the results of the subtraction. If the linearity is sufficiently good, there would be no difference between the two images. However, significant departures from the zero level appear when the count is higher than 10,000e$^-$ in both the CCD chips. The count difference can be clearly expressed as a single function of the count level for the entire area in each CCD chip. This indicates that our assumption that the nonlinearity effect is not dependent on the pixels is reasonable.

We derive a formula to quantify the nonlinearity effect by fitting this relation between the count level and the count difference. As mentioned above, figure 4 shows the count difference (dL) between the measured apparent counts, [f ($t_{\rm exp}$)], for two different exposure times, $t_{\rm exp}$ (30 s and 60 s); in this case, the errors caused by the nonlinearity are included:

$$dL = f(60) - \frac{60}{30} \cdot f(30) \quad . \tag{1}$$

We assume that the apparent count is obtained for the values expected for the perfect linearity case, [$F(t_{\rm exp})$]:

$$f(t_{\rm exp}) = F(t_{\rm exp}) + \Delta R[F(t_{\rm exp})] \quad , \tag{2}$$

where $\Delta R[F(t_{\rm exp})]$ indicates the departure from linearity. $\Delta R[F(t_{\rm exp})]$ is considerably smaller than $F(t_{\rm exp})$ and is approximated as $\Delta R[f(t_{\rm exp})]$. The apparent count for the 30-s exposure can be expressed as

$$f(30) = F(30) + \Delta R[F(30)] \tag{3}$$

$$= \frac{F(60)}{2} + \Delta R\left(\frac{F(60)}{2}\right) \tag{4}$$

$$\sim \frac{F(60)}{2} + \Delta R\left(\frac{f(60)}{2}\right) \tag{5}$$

Then, dL is expressed as

$$dL(x) = \Delta R(x) - 2 \cdot \Delta R(x/2) \quad , \tag{6}$$

where x is $f(60)$.

If $\Delta R(x)$ is assumed to be given as a polynomial

$$\Delta R(x) = \sum_{i=0} A_i \cdot x^i \quad , \tag{7}$$

dL can be written as

$$dL(x) = -A_0 + \sum_{i=2} A_i \cdot \left(1 - \frac{1}{2^{i-1}}\right) \cdot x^i \tag{8}$$

$$= B_0 + B_2 x^2 + B_3 x^3 + B_4 x^4 + \cdots \quad . \tag{9}$$

The coefficients B_i are derived by fitting to the data, as shown in figure 4. For the frames with bias level correction,

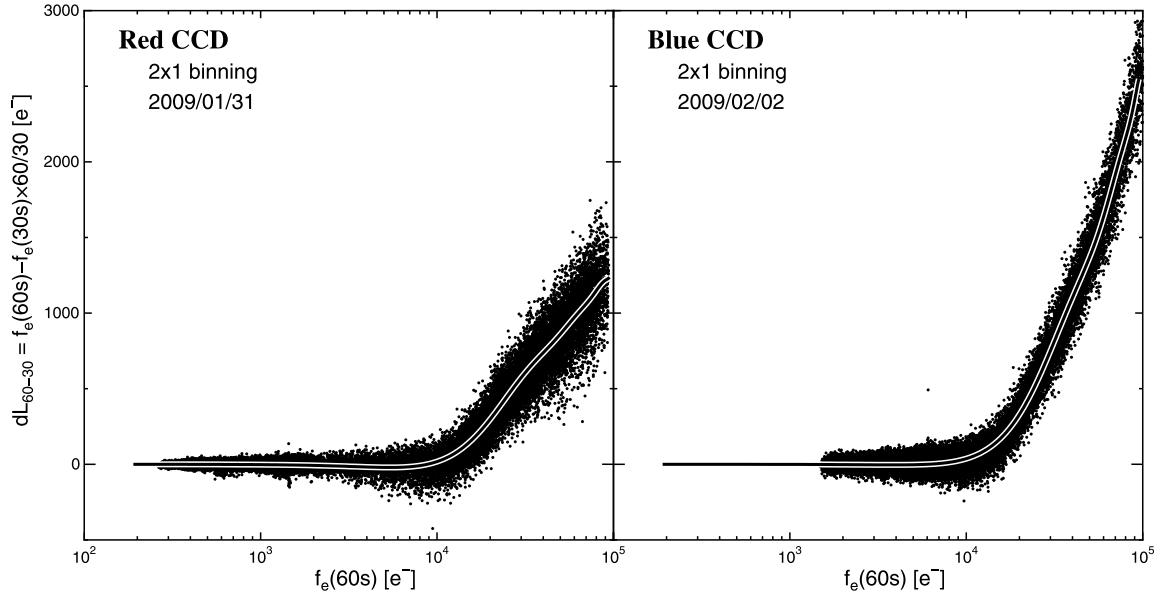

Fig. 4. Count difference (dL_{60-30}) measured from the apparent counts at exposure times of 60 s and 30 s. The left (right) panel shows the result obtained for the red (blue) CCD in the 2×1 (spatial×wavelength) binning mode. Solid lines show the fitting results for each measurement point; fitting is performed with ninth-order polynomials. Nonlinearity effects are clearly observed for electron numbers greater than 10,000e$^-$ in both the CCD chips.

B_0 ($= -A_0$) must be negligible. The CCD count after nonlinearity correction is given as

$$F(x) = x - \sum_{i=2} \frac{2^{i-1}}{2^{i-1}-1} \cdot B_i x^i \quad . \tag{10}$$

In figure 4, the fitting results are shown by solid lines; fitting is made for B_i for $i = 2$ to 9. Figure 5 shows the results after the corrections; this figure indicates that our correction procedure is fairly effective. The residual trend in the corrected data (dL_{60-30}) is approximately 100e$^-$ for the red CCD and 300e$^-$ for the blue CCD at 100,000e$^-$. These values correspond to relative errors of 0.02% and 0.05%, respectively, in the case of perfect linearity. It is apparent that since these errors are caused by the Poisson noise, they are reduced when the CCD count decreases. The above formula can be adopted to all other pairs of exposure times, in which one exposure time is twice the other. Indeed, the correction performance is also confirmed for the other sets of exposure times (e.g., 25 s and 50 s) by our measurements. Hence, x[$= f(60)$] in equation (10) can be replaced with the apparent CCD count for any exposure time (F_{raw}). The corrected CCD count (F_{cor}) for F_{raw} is given as

$$F_{cor} = F_{raw} - \sum_{i=2} \frac{2^{i-1}}{2^{i-1}-1} \cdot B_i F_{raw}^i \quad . \tag{11}$$

The fitting curves (solid lines) in figures 4 and 5 do not indicate the correction factors for nonlinearity because the values shown in the figures are not the CCD counts but the dL values. The correction curves for the CCD counts (equation [11]) derived from the fitting curves are shown by dotted lines in figure 5.

The departure from linearity occurs from ~10,000e$^-$ and rapidly increases thereafter. The departure becomes 3,000e$^-$ at 50,000e$^-$, i.e., 6%, for the red CCD. This value appears to be greater than that shown in figure 3 (maximum 4%). However, these departure values are dependent on the fitting procedure, that is, on the count range in which the weight of the fitting is obtained. In figure 3, the fitting is essentially determined for the range with high CCD counts, while in figures 4 and 5, the fitting is determined from the low CCD counts.

Snellen et al. (2008) empirically estimated the nonlinearity effect in HDS CCDs, indicating that an increase of 2–3% in the apparent count when ADU approaches 10,000; $F_{cor} = (1.0 - 0.03 \times F_{raw}/10^4) F_{raw}$ for the red CCD. This is consistent with our result obtained for electron numbers lower than 17,000e$^-$ (~10,000 ADU), and the error is within 1.5%. However, this estimation cannot be adopted for higher counts. Our method helps achieve improved correction for a very wide range of data counts, from 0e$^-$ to 100,000e$^-$.

3. Results and Discussion

The CCD data obtained for the HDS are read out from the two ports for each CCD chip. We applied this correction technique separately to two regions in each CCD chip corresponding to the two readout ports and found no significant difference between the two regions. In contrast,

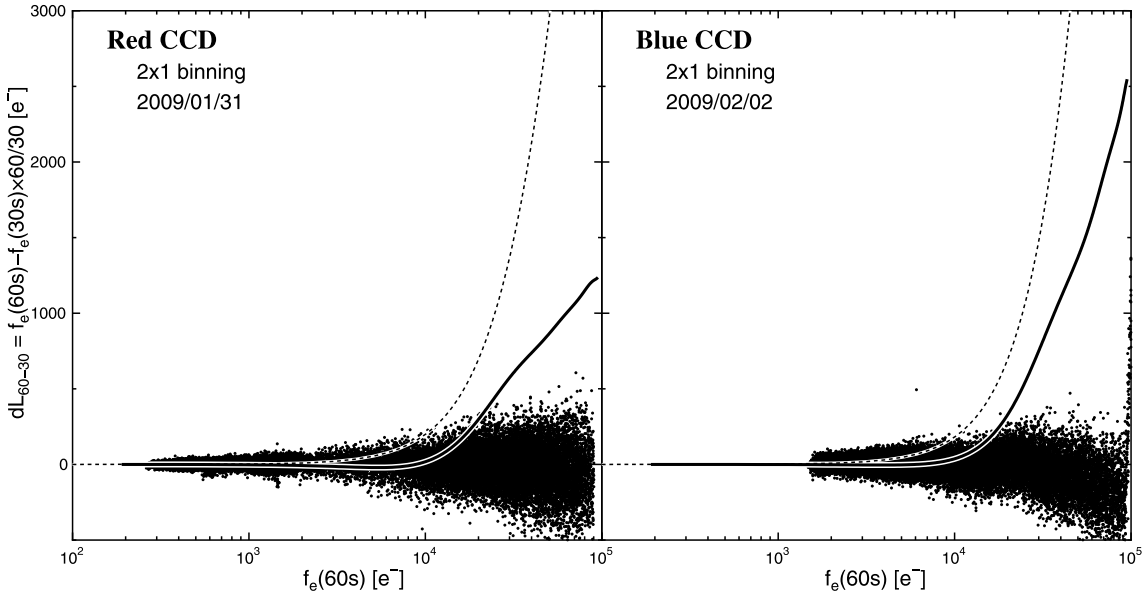

Fig. 5. Count difference (dL_{60-30}) after our correction. Solid lines are the same as those ones in figure 4. Dotted lines show the correction curves ($F_{raw} - F_{cor}$) derived from the fitting curves shown by solid lines. Corrected data show a very flat dL for all the count, indicating that the correction is valid up to 100,000e$^-$.

the correction parameters are clearly different between the two CCD chips used in the HDS (see figure 5). Hence, we can not obtain the conditions for distinguishing the two possible source of nonlinearity (the CCD chip or the electronics). This is because the two CCDs are driven by different electronics.

We also investigate the dependence of the nonlinearity on the binning modes. We measure the coefficients B_i in equation (9) for all combinations of CCD chips (red and blue) with different binning modes (spatial × wavelength: 1×1, 2×1, 2×2, 2×4, 4×1, and 4×4). In order to maintain the signal counts in each binning mode at the same level, we adjust the slit width for each measurement. The results are listed in table 1 along with the correlation coefficients, $|r|$, standard deviations of dL_{60-30}, σ, and the dates on which the measurements are obtained for each fitting. Figure 6 shows the fitting results obtained for the dL values for different binning modes. There are differences between the dL values obtained in different binning modes; however, these differences are clearly smaller than those found between the two CCD chips. In particular, the results are almost identical for the modes with the same spatial direction binning (2×1, 2×2, and 2×4 in the figure). The correction coefficients (B_i) are provided for each binning mode in table 1.

For two years (July 2007 to May 2009), the same measurements were repeated 10 times for both CCD chips, mainly in the 2×1 binning mode, which is most frequently used for actual observations. No clear variation in the nonlinearity effect was detected (< 0.01% in dL_{60-30}).

We applied our correction method to an actual stellar spectrum with a very high count (~33,000e$^-$) and insufficient spatial sampling (4×1 binning). As shown in figure 7 (left panel), the pretended "beats" in the continuum of a rapidly rotating star appear due to the problem as mentioned in section 1. The "beats" are clearly removed after the correction for nonlinearity (right panel of figure 7).

The effect of nonlinearity on the actual observational data collected to date does not appear to be significant in most HDS observations; this is because electron numbers greater than 10,000e$^-$ have not been achieved in most cases during one exposure. However, in some special cases that require a very high SNR, the linearity correction derived from our measurements must be adopted for each frame. Since no clear time variation is found in the nonlinearity effect, the B_i values in table 1 can be used for every HDS frame depending on the CCD chip and the binning mode. In an actual data analysis, this correction can be easily applied by using a single task of the IRAF reduction package (e.g.,images/imutil/imexpr). An IRAF script in which all the coefficients B_i are included is available on the website of the Subaru/HDS. It should be noted that the current CCD controller (Messia-V) was installed in March 2004. The corrections given here can be applied to the data obtained after this upgrade.

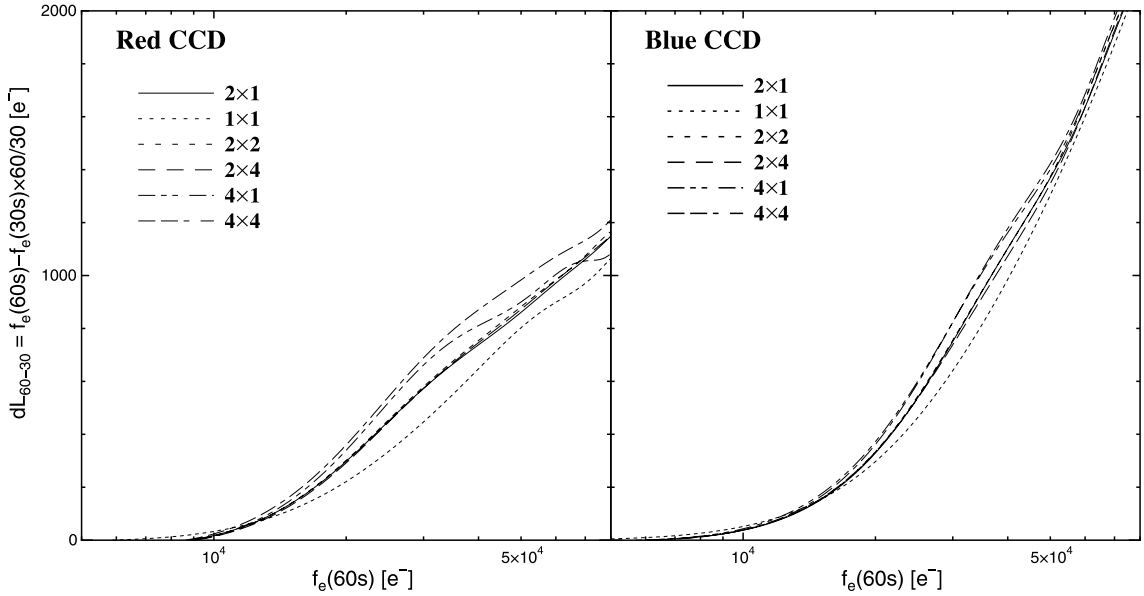

Fig. 6. Fitting results for dL, shown in equation (9). The differences between the results for various binning modes are considerably smaller than the difference between the red and the blue CCD chips. In particular, the curves for 2×1, 2×2, and 2×4 binning are in good agreement for both chips.

Table 1 Coefficients B_i for each CCD chip for different binning modes.

	Red CCD					
	1×1	2×1	2×2	2×4	4×1	4×4
B_2	−9.6823939e−07	−2.7629947e−06	−3.1226151e−06	−2.8528732e−06	−2.8167430e−06	−3.1641202e−06
B_3	2.3434520e−10	5.1440847e−10	5.8252838e−10	5.2087438e−10	4.9245638e−10	5.9223507e−10
B_4	−1.4175356e−14	−2.9215381e−14	−3.4269779e−14	−2.9445433e−14	−2.4512440e−14	−3.3274607e−14
B_5	4.4542967e−19	8.4490112e−19	1.0399943e−18	8.5280778e−19	5.7702891e−19	9.4739949e−19
B_6	−8.1763008e−24	−1.4021438e−23	−1.8265468e−23	−1.4240244e−23	−6.9786360e−24	−1.5449714e−23
B_7	8.7749327e−29	1.3532646e−28	1.8763189e−28	1.3884683e−28	3.9091775e−29	1.4629632e−28
B_8	−5.0860064e−34	−7.0746507e−34	−1.0478168e−33	−7.3595199e−34	−4.2969340e−35	−7.4897020e−34
B_9	1.2273852e−39	1.5505315e−39	2.4582068e−39	1.6407086e−39	−2.8403124e−40	1.6039831e−39
$\|r\|$	0.97045886	0.97179847	0.97641471	0.97529335	0.97772020	0.97908163
σ	72.119377	80.225602	75.022239	76.595253	74.624315	79.974977
date	02-03-2009	01-31-2009	02-03-2009	02-03-2009	02-03-2009	02-03-2009

	Blue CCD					
	1×1	2×1	2×2	2×4	4×1	4×4
B_2	−3.8367214e−07	−8.3128848e−07	−7.2850038e−07	−1.0278111e−06	−9.1789776e−07	−9.2670609e−07
B_3	1.4620104e−10	1.6613441e−10	1.4636319e−10	2.0759443e−10	1.8148583e−10	1.7101338e−10
B_4	−7.1203412e−15	−4.7080893e−15	−2.9742925e−15	−7.6242810e−15	−4.4087838e−15	−3.5228211e−15
B_5	1.7216029e−19	−3.3782728e−21	−8.0584724e−20	9.2266191e−20	−5.9936799e−20	−8.6687757e−20
B_6	−2.4041836e−24	2.1982253e−24	4.0469784e−24	5.2346784e−25	4.0361619e−24	4.4032595e−24
B_7	1.9623589e−29	−3.9795147e−29	−6.3861521e−29	−2.3577454e−29	−6.6444272e−29	−6.8545547e−29
B_8	−8.6702747e−35	2.9406962e−34	4.5426672e−34	2.1182827e−34	4.7850548e−34	4.7937480e−34
B_9	1.5957180e−40	−8.1006694e−40	−1.2367311e−39	−6.3899159e−40	−1.3063059e−39	−1.2824365e−39
$\|r\|$	0.98954012	0.99070936	0.99081607	0.99086189	0.99110285	0.99188753
σ	71.397778	70.217478	70.847602	69.410816	69.331226	68.880542
date	02-03-2009	02-03-2009	02-03-2009	05-15-2009	05-14-2009	02-03-2009

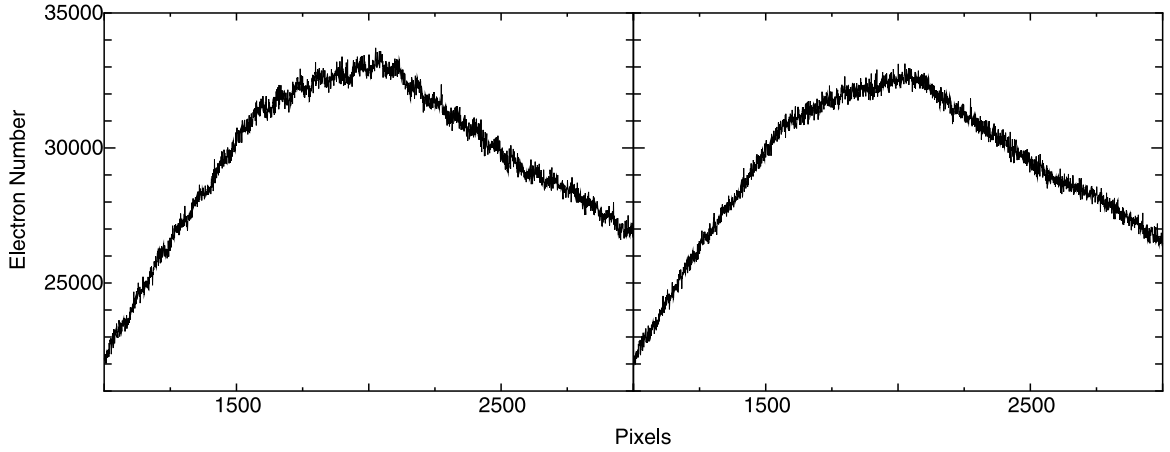

Fig. 7. Application of the correction method to a spectrum of a rapidly rotating star with a very high count obtained with insufficient spatial sampling. Data obtained in the 4×1 binning mode, in which 1 binned pixel corresponds to 0″.55 in the spatial direction, under the ∼0″.4 seeing conditions. The left panel shows resultant spectrum after the removal of the overscan region, bias level correction, conversion from ADU counts to electron numbers, and aperture extraction. The right panel shows the spectrum obtained by applying our linearity correction to the same data before the aperture extraction. The spectrum without correction (left panel) has pretended "beats", whose maximum amplitude is approximately 700e^- (∼2% of the continuum level). However, they are removed in the corrected spectra (right panel).

4. Summary

We investigate the nonlinearity of the CCDs used in the Subaru/HDS. Our measurements reveal that the nonlinearity of the HDS CCDs becomes significant for electron numbers greater than 10,000e^-, both in the red and blue CCD chips. The nonlinearity becomes high (several percent) at 50,000e^-. The nonlinearity characteristics are independent of the pixels in each CCD. The nonlinearity differs considerably between the two CCD chips.

Using the variations in the CCD counts in each spectral image, we derive a correction function for this nonlinearity by a simple method. This method considers several (typically 10) pairs of flat spectra recorded at two different exposure times (60 s and 30 s). This method is highly advantageous since it facilitates rapid measurements and helps achieve high accuracy in the correction curve obtained for a large number of measurement points. This measurement technique is expected to be useful for investigating the nonlinearity of detectors in general.

We are grateful to Dr. Hideyuki Izumiura for his valuable comments upon this work. N.N. is supported by the Japan Society for Promotion of Science (JSPS) Fellowship for Research (PD: 20-8141).

REFERENCES

Izumiura, H. 1999, in *Proceedings 4th East Asian Meeting on Astronomy*, ed. P. S. Chen (Kunming: Yunnan Observatory), 77.

Izumiura, H. 2008, private communication.

Nakaya, H., Komiyama, Y., Miyazaki, S., Yamashita, T., Yagi, M., & Sekiguchi, M. 2006, *PASP*, **118**, 478.

Noguchi, K., et al. 2002, *PASJ*, **54**, 855.

Sekiguchi, M., Nakaya, H., Kataza, H., & Miyazaki, S. 1998, *Exp. Astron.*, **8**, 51.

Snellen, I. A. G., Albrecht, S., de Mooij, E. J. W., & Le Poole, R. S. 2008, *A&A*, **487**, 357.

Worswick, S. P., Gellatly, D. W., Ferneyhough, N. K., King, D. L., Weise, A. J., Bingham, R. G., Oates, A. P., 1995, *Proc. SPIE*, **2476**, 46.